RSC Advances

ROYAL SOCIETY OF CHEMISTRY

www.rsc.org/advances

Direct co-culture of endothelial and smooth muscle cells on poly(ε-caprolactone) nanowire surfaces

Victoria Leszczak[1] and Ketul C. Popat[1,2,*]

[1] Department of Mechanical Engineering, Colorado State University, Fort Collins CO 80523

[2] School of Biomedical Engineering, Colorado State University, Fort Collins CO 80523

* Author of correspondence: ketul.popat@colostate.edu

ABSTRACT

Current cardiovascular implants cause restenosis, calcification and thrombosis due to insufficient integration with native tissue. A thorough understanding of the interaction between the cells and the biomaterial involved is fundamental in a successful implant that promotes healing and tissue regeneration. In this study, we have developed collagen-immobilized nanostructured surfaces from poly(ε-caprolactone) for the growth and maintenance of co-cultures of endothelial and smooth muscle cells. Cell adhesion, morphology and differentiation was investigated using microscopy and western blotting. The results presented here indicate that collagen-immobilized nanostructured surfaces may be good interfaces for use in cardiovascular applications and warrants further investigation.

1. Introduction

Stents and vascular grafts have been used routinely for the treatment of cardiovascular diseases. Prosthetic materials such as polyethylene terephthalate, polytetrafluoroethylene (PTFE), expanded PTFE and polyurethane are common materials used for cardiovascular implants [1]. Unfortunately these materials have limited re-endothelialization potential, promoting thrombosis, restenosis and infection once implanted, eventually leading to implant failure resulting in further interventions [2]. Cardiovascular tissue requires interactions between the endothelial cells (ECs) and the underlying smooth muscle cells (SMCs), vital for cardiovascular health and important for normal function of blood vessels [3,4]. The communication between these cells, an essential aspect of natural maintenance of tissue and a number of pathophysiological responses, is disrupted upon implantation of a cardiovascular biomaterial [5]. Any damage to the EC layer following implantation exposes the underlying sub-endothelial extracellular matrix, promoting thrombus formation, inflammation and SMC proliferation, thus demonstrating the importance of re-establishing or maintaining the integrity of the EC layer and EC-SMC communication.

ECs and SMCs act as a linked system for the communication of signals from receptors confined on the endothelium surface to the vessel wall and vice versa. It has been shown that bidirectional electrical signals flow in response to kinins between ECs and SMCs [6]. ECs and SMCs in the vascular wall can communicate through the release of signals into the surrounding medium, or via direct cell-cell contact through junctions formed between the cells [7]. ECs respond to environmental cues by producing both growth inhibitors and stimulators of SMCs, affecting SMCs both *in vivo* and *in vitro*. In particular, nitric oxide (NO) released by ECs is responsible for inhibiting the proliferation of SMCs via the extracellular signal-regulated kinase (ERK)

pathway [8]. Studies have also shown that the rate of proliferation of SMCs is directly dependent on the state of endothelium [9]. When the endothelium is in a confluent state, the normal growth rate of SMCs is completely inhibited. Further, ECs cultured with synthetic state SMCs separated by a porous membrane demonstrated increased EC adhesion molecule expression, suggesting that synthetic SMCs activate the endothelium [10]. Therefore a specific ratio of ECs to SMCs and maintenance of a differentiated cellular state is vital to healthy cardiovascular tissues.

An intact endothelium at the vessel-biomaterial interface is fundamental in preventing thrombosis and over-proliferation of the SMCs. However, current biomaterial surfaces used for cardiovascular implants are incapable of re-endothelialization, causing these adverse effects by disrupting normal communication between ECs and SMCs. Previous studies have attempted to prevent thrombosis and restenosis induced by SMC proliferation by incorporating drugs on the surface of cardiovascular implants. Three drugs: heparin, sirolimus, and paclitaxel, have been investigated for treating and/or preventing restenosis [11]. However, drug eluting cardiovascular implants require longer treatment with blood thinners to prevent sudden stent closure from clotting. Previous research has shown that stents seeded with ECs before being implanted can inhibit thrombosis and neointimal hyperplasia [12, 13]. However, very few studies have looked at providing nanotopography on implant surface to stimulate proper communication between ECs and SMCs [14, 15].

In this study, we have investigated co-cultures of ECs and SMCs on nanostructured surfaces fabricated from poly(ε-caprolactone), a polymer often used in artificial vessel development [16-18]. By using a simple nanotemplating technique, nanotopography similar to the features within the natural extracellular matrix of cardiovascular tissue was introduced. The surface was immobilized with collagen, a key component of vascular tissue. Human

microvascular ECs and human aortic SMCs were used to investigate the ability of collagen-immobilized poly(ε-caprolactone) nanostructured surfaces to maintain differentiated phenotypes. Previous studies have demonstrated an enhanced EC and SMC response on these nanostructured surfaces, promoting the differentiation of both ECs and SMCs when cultured individually [19, 20], however not much is known about how these cells will interact in a co-culture environment, and hence was investigated in this study.

2. Materials and Methods

2.1. Fabrication of surfaces

Surfaces were fabricated and characterized as described previously [19-21]. In brief, control (PCL) surfaces were fabricated by sintering polycaprolactone pellets on a glass plate in a 10 mm Teflon washer. Polycaprolactone nanowire surfaces (NW) were fabricated using a solvent free nanotemplating technique with 20 nm diameter nanoporous aluminum oxide membranes [22]. The nanowires were gravimetrically extruded through the membrane and the aluminum oxide membranes were dissolved in 1 M NaOH for 75 mins. The surfaces were then washed in DI water (3x), dried and stored in a desiccator until their use was required.

Prior to any further use, all surfaces were sterilized in 70 % ethanol for 30 mins, followed by a PBS rinse (2x). The surfaces were then air dried and further sterilized by UV exposure for 30 mins.

2.2. Immobilization of collagen on PCL and NW surfaces.

PCL and NW surfaces were immobilized with collagen in three successive steps [23]. First, the surfaces were subjected to aminolysis by incubation in 1,6-hexanediamine/2-propanol

(6 % w/v) for 10 mins at 37 ºC. This was followed by rinsing (3x) with DI water to remove excess and unreacted 1,6-hexanediamine. Second, the surfaces were incubated in a gluteraldehyde (1 wt%) solution at 2-4 °C for 24 hrs and rinsed (3x) with DI water to remove excess gluteraldehyde. Third, the surfaces were placed in a type I collagen solution (1 % w/v) for 24 hrs at 2-4 °C. After the incubation, the surfaces were rinsed with 0.1 M acetic acid solution to remove ungrafted collagen, followed by a DI water rinse (3x).

Notation for different surfaces in the rest of this communication is as follows: Control (PCL), Control + Collagen (cPCL), Nanowire (NW), Nanowire + Collagen (cNW).

2.3. Characterization of surfaces.

The surface architecture was characterized using scanning electron microscopy (SEM). Prior to imaging, surfaces were coated with 10 nm of gold. Surfaces were imaged at 7 kV and surface morphology was investigated to ensure topographies were similar before and after collagen immobilization.

The surface composition was analyzed using X-ray photospectroscopy (XPS). Survey scans were taken before and after collagen immobilization, in order to determine the overall composition of the different surfaces.

2.4. Human Aortic Smooth Muscle Cell and Human Microvascular Endothelial Cell Culture

Both human aortic SMCs (Life Technologies) and human microvascular ECs were suspended in MCDB 131 media (Life Technologies) enhanced with SMC growth supplement (Life Technologies) or microvascular growth supplement (Life Technologies), respectively (both supplemented with 2 mmol/l glutamine, 100 ug/ml penicillin, and 100 ug/ml

streptomycin) and added to 75 cm^2 culture flasks and incubated at standard culture conditions. This study was performed using SMCs that were passage 4 and ECs at passage 5.

Prior to seeding, all surfaces were subjected to 30 min UV exposure and conditioned in culture medium. To investigate cellular response to difference surfaces, first, SMCs were cultured on PCL, NW, cPCL and cNW surfaces in a 48-well plate. The SMCs were seeded at a high density of 5×10^6 cells/well. This cell density was chosen to promote initial adhesion and quick confluency. The surfaces were incubated in standard culture conditions in 400 µl of cell rich medium and allowed to adhere for 24 hrs. After 24 hrs in culture, the ECs were seeded at a similar density of 5×10^6 cells/well on top of the adhered SMCs. After 24 hrs of co-culture, media changes were done with MCDB 131 media enhanced with SMC differentiation supplement (supplemented with 2 mmol/l glutamine, 100 ug/ml penicillin, and 100 ug/ml streptomycin). Cellular adhesion and morphology was investigated after 7 days in culture. Cellular differentiation was investigated after 7 and 14 days in culture.

2.5. Adhesion of EC and SMC on different surfaces

Cell adhesion was investigated by staining cells with rhodamine phalloidin (Cytoskeleton) and 4′,6-diamidino-2-phenylindole dihydrochloride (DAPI) (Invitrogen) nucleus stain followed by fluorescence microscope imaging after 7 days in culture.

Prior to staining non-adherent cells were removed by aspirating the cell rich medium from the surfaces followed by two gentle rinses with PBS. The surfaces were then transferred to a new 48-well plate and fixed with 3.7% formaldehyde 15 mins at room temperature. This was followed by a PBS rinse, followed by incubating the surfaces in 1 % Triton-X 100 for 3 mins in order to permeabilize the cells. The surfaces were rinsed in PBS and transferred to a new 48-

well plate, then incubated in rhodamine-phalloidin at a concentration of 5 µL/mL (14 μM stock) for 30 mins. DAPI (300 nM) was added after 25 mins. All the surfaces were rinsed with PBS and imaged with a fluorescence microscope (Zeiss).

2.6. Morphology of EC and SMC on different surfaces

The cell morphology was investigated using SEM imaging to visualize the cellular interaction with the surface nanoarchitecture. The non-adherent cells were removed by aspirating the media and unadhered cells from the surfaces followed by two gentle rinses with PBS. The surfaces were then transferred to a clean petri dish where the cells were fixed and dehydrated. The cells were fixed by incubating the surfaces in a solution of primary fixative (3 % glutaraldehyde (Sigma), 0.1 M sodium cacodylate (Polysciences), and 0.1 M sucrose (Sigma)) for 45 min. They were then incubated in a solution of secondary fixative (primary fixative without gluteraldehyde) for 10 min. Subsequently, the surfaces were dehydrated by incubation in consecutive solutions of increasing ethanol concentrations (35 %, 50 %, 70 %, 95 %, and 100 %) for 10 min each. Further dehydration of the cells was accomplished by incubating the surfaces in hexamethyldisilazane (HMDS, Sigma) for 10 min. They were then air dried and stored in a desiccator until further imaging by SEM. The surfaces were coated with a 10 nm layer of gold and imaged at 7 kV.

2.7. Differentiation of EC and SMC on different surfaces

Western blotting was performed to identify the expression of EC and SMC specific differentiation proteins, VE-cadherin and heavy chain myosin (MYH) respectively. Further, non-muscle specific myosin IIB (SMemb), a marker of undifferentiated and proliferating SMCs was

blotted for. Briefly, cells on surfaces after 7 and 14 days in culture were homogenized in RIPA lysis buffer (10.0 mM Tris pH 7.4, 100.0 mM NaCl, 5.0 mM EDTA, 5.0 mM EGTA, 1.0% Deoxycholate, 0.1% SDS, 1.0% Triton X-100), also containing protease inhibitor cocktail. The lysate protein content was determined by micro-BCA assay. The lysate was heated to 65 °C for 10 mins in sample buffer (62.5 mM Tris-HCl pH 6.8, 10.0 % glycerol, 5.0 % β-mercaptoethanol, 2.0% SDS, 0.025 % Bromophenol blue) in order to denature the proteins prior to gel loading. Approximately 25 μg of total extract protein was electrophoresed through 8 % Tris-SDS gels and transferred to PVDF membranes in 7.5% methanol. Blots were blocked for 1 hr at room temperature. Primary monoclonal antibodies for VE-cadherin, MYH or SMemb were diluted 1:500 in 3% BSA in PBS-tween solution and incubated overnight at 4 °C. The PVDF membranes were then washed three times with PBS-tween solution (5 mins per wash) before they were incubated with goat anti-mouse or donkey anti-rabbit horseradish peroxidase (HRP) conjugated secondary antibodies (Santa Cruz Biotechnology) at a dilution of 1:5000 for 1 hr at room temperature. The PVDF membranes were then washed three times with PBS-tween solution (5 mins per wash) followed by protein detection using chemiluminescence (WestPico Chemiluminescent Substrate; Pierce). The PVDF membranes were imaged using an Alpha Innotech Fluorchem gel documentation system, and band intensities were analyzed using ImageJ software.

3. Results and Discussion

Current biomaterial surfaces used for cardiovascular implants are incapable of re-endothelialization, causing adverse effects by disrupting normal communication between ECs and SMCs. In this study, we have investigated the co-culture of ECs and SMCs on collagen

immobilized polycaprolactone nanowire surfaces. In order to provide insights into the material surfaces' feasibility for use as an interface in cardiovascular applications, human microvascular ECs and human aortic SMCs were used.

3.1. Characterization of Surfaces

The surface architecture of the different surfaces before and after the collagen immobilization process was characterized using SEM. Results reveal that surface architecture remains consistent before and after collagen immobilization (**Fig. 1**).

The surface composition of the surfaces was analyzed using X-ray photoelectron spectroscopy (XPS). Survey scans were taken before and after collagen immobilization in order to determine the overall composition of the different surfaces. Results indicate an increase in the N1s peak after the after collagen immobilization on both PCL and NW surfaces (**Table 1**).

3.2. Adhesion of ECs and SMCs on different surfaces

The adhesion of EC and SMC co-cultures on different surfaces was investigated after 7 days in culture by using Rhodamine Phalloidin (Cytoskeleton) and 4′,6-diamidino-2-phenylindole dihydrochloride (DAPI) (Invitrogen) nucleus stain, followed by imaging with a fluorescence microscope (**Fig. 2**). Results indicate that NW, cPCL and cNW surfaces are confluent with cells, unlike PCL surfaces that are not confluent with cells. It is well known that both SMCs and ECs adhere better to either nanostructured surfaces and/or bioactive surfaces [15, 24-26]. However, due to lack of these features on PCL surfaces, the cells did not reach confluency. Further, cells on all surfaces appear to be aligning and have a "spindle" shape. SMCs are incredibly plastic and are known to exhibit two different phenotypes depending on their

environment: a synthetic phenotype and a contractile phenotype [27]. Synthetic SMCs exhibit an epithelioid morphology, linked to high rates of proliferation. Contractile SMCs are elongated and spindle shaped, and also associated with low proliferative activity. Further, ECs are also known to have elongated morphology *in vivo*. The high magnification fluorescence microscopy images show elongated and spindle shape morphologies of cells indicating that most of the cells on the surfaces are either contractile SMCs or normal ECs. The images also show cellular filopodia interactions with surrounding cells on all surfaces.

3.4. Morphology of EC and SMC on different surfaces

The cell morphology was investigated using SEM imaging to visualize the cellular interaction with the surface nanoarchitecture. The results indicate that NW, cPCL and cNW surfaces are confluent with cells (**Fig. 3**). Similar to fluorescence imaging results, high magnification images show cellular filopodia interactions with surrounding cells on all the surfaces. Further, co-cultures on NW, cPCL and cNW surfaces appear more spindle-shaped (contractile-appearing phenotype), with more evenly distributed cells.

3.5. Differentiation of SMC and EC co-cultures on different surfaces

The differentiation of ECs and SMCs in co-culture on surfaces was investigated by detecting VE-cadherin, MYH and SMemb expression through western blotting techniques after 7 and 14 days in culture. Both VE-cadherin and MYH are specific to a differentiated EC and SMC phenotype, respectively. VE-cadherin expression is important in EC contacts, which will eventually regulate the permeability of the blood vessel, thus an increase in VE-cadherin expression is necessary for healthy vasculature. MYH expression is an end-state differentiation

marker highly specific to SMCs. SMemb is also expressed in SMCs undergoing growth and/or cell division, such as proliferating (undifferentiated, synthetic) SMCs [28]. The results indicate that VE-cadherin expression is significantly higher on PCL and NW surfaces after 7 days in culture compared to cPCL and cNW surfaces (**Fig. 4**). However, the expression of VE-cadherin after 14 days in culture decreases on both PCL and NW surfaces. VE-cadherin expression on collagen immobilized surfaces increases significantly from 7 days in culture to 14 days in culture, indicating an increase in the amount of EC cell-cell junctions formed via VE-cadherin.

MYH expression is significantly higher on NW, cPCL and cNW surfaces after 7 and 14 days in culture compared to PCL surfaces. However, MYH expression significantly decreases on NW, cPCL and cNW surfaces from 7 days in culture to 14 days in culture (**Fig. 4**), while no significant difference was seen in MYH expression on PCL surfaces from 7 days in culture to 14 days in culture. These results suggest that SMCs might be switching to a synthetic phenotype and proliferating on NW, cPCL and cNW surfaces, or that the SMCs are differentiated. Once SMCs are in a differentiated state, their proliferation rates are significantly lower which would account for the decrease in MYH expression normalized to α-tubulin on NW, cPCL and cNW surfaces. α-tubulin is present in the microtubules of both ECs and SMCs. This conclusion is further supported by the significant decrease in SMemb expression on all surfaces from 7 days in culture to 14 days in culture, indicating that a significant amount of SMCs are not switching to a synthetic phenotype (**Fig. 4**).

Studies have shown that SMCs and ECs exhibit favorable interactions when co-cultured [29-31]. By incorporating nanotopography or a cell binding motif, more ECs and SMCs are able to attach and interact, thus explaining the increased expression of differentiation proteins specific to

ECs and a decrease in SMC synthetic state markers on NW, cPCL and cNW surfaces compared to PCL surfaces.

3. Conclusions

Cardiovascular tissue requires interactions between the endothelium with the underlying SMCs, which is vital for cardiovascular health and is considered to be important in the functions of blood vessels. In this study, we have investigated EC and SMC co-cultures on collagen-immobilized poly(ε-caprolactone) nanostructured surfaces. It is important to understand how ECs and SMCs interact together on these surfaces in order to have a successful cardiovascular implant. Fluorescence microscopy and SEM images reveal that NW, cPCL and cNW surfaces are confluent with cells. Further, ECs and SMCs on these surfaces seem to be more aligned and more spindle-shaped (contractile-appearing phenotype), with more evenly distributed cells. Western blotting results reveal that there is a significant increase in VE-cadherin expression after 14 days in culture on NW and cNW surfaces. MYH expression decreases on NW, cPCL and cNW surfaces from day 7 to day 14 in culture. The decrease in MYH expression can be attributed to the decrease in proliferation of differentiated SMCs. This is confirmed by the significant decrease in SMemb, an undifferentiated, synthetic state SMC marker, from day 7 to day 14 in culture. After 14 days in culture MYH expression is significantly higher on NW, cPCL and cNW surfaces compared to PCL surfaces. These combined results indicate that collagen-immobilized nanostructured surfaces may be good interfaces for use in cardiovascular applications and warrants further investigation.

Acknowledgements

Research reported in this publication was supported by the National Institute of Arthritis and Musculoskeletal and Skin Diseases of the National Institutes of Health under Award Number 5-R21-AR057341-02. The content is solely the responsibility of the authors and does not necessarily represent the official views of the National Institutes of Health.

References:

1. B. O'Brien and W. Carroll, *Acta Biomaterialia*, 2009, **5**, 945-958.
2. A. de Mel, G. Jell, M. M. Stevens and A. M. Seifalian, *Biomacromolecules*, 2008, **9**, 2969-2979.
3. P. A. Jones, *Proceedings of the National Academy of Sciences of the United States of America*, 1979, **76**, 1882-1886.
4. S. M. Vernon, M. J. Campos, T. Haystead, M. M. Thompson, P. E. DiCorleto and G. K. Owens, *The American journal of physiology*, 1997, **272**, C582-591.
5. R. A. Rossello and D. H. Kohn, *Commun Integr Biol*, 2010, **3**, 53-56.
6. *Bidirectional electrical communication between smooth muscle and endothelial cells in the pig coronary artery*, 1994.
7. M. F. Fillinger, L. N. Sampson, J. L. Cronenwett, R. J. Powell and R. J. Wagner, *Journal of Surgical Research*, 1997, **67**, 169-178.
8. U. Förstermann, *Pflugers Arch - Eur J Physiol*, 2010, **459**, 923-939.
9. B. S. Zuckerbraun, D. A. Stoyanovsky, R. Sengupta, R. A. Shapiro, B. A. Ozanich, J. Rao, J. E. Barbato and E. Tzeng, *Am J Physiol Cell Physiol.*, 2007, **292**, C824-831. Epub 2006 Aug 2016.
10. J. J. Chiu, L. J. Chen, C. I. Lee, P. L. Lee, D. Y. Lee, M. C. Tsai, C. W. Lin, S. Usami and S. Chien, *Blood*, 2007, **110**, 519-528.
11. T. Parker, V. Dave and R. Falotico, *Current pharmaceutical design*, 2010, **16**, 3978-3988.
12. D. A. Dichek, R. F. Neville, J. A. Zwiebel, S. M. Freeman, M. B. Leon and W. F. Anderson, *Circulation*, 1989, **80**, 1347-1353.
13. T. Shirota, H. Yasui, H. Shimokawa and T. Matsuda, *Biomaterials*, 2003, **24**, 2295-2302.
14. Y. Liu, S. Rayatpisheh, S. Y. Chew and M. B. Chan-Park, *ACS applied materials & interfaces*, 2012, **4**, 1378-1387.
15. C. J. Bettinger, Z. Zhang, S. Gerecht, J. T. Borenstein and R. Langer, *Advanced Materials*, 2008, **20**, 99-103.
16. K. Wulf, M. Teske, M. Lobler, F. Luderer, K. P. Schmitz and K. Sternberg, *Journal of biomedical materials research. Part B, Applied biomaterials*, 2011, **98**, 89-100.
17. M. R. Williamson, K. J. Woollard, H. R. Griffiths and A. G. Coombes, *Tissue engineering*, 2006, **12**, 45-51.
18. S. de Valence, J.-C. Tille, D. Mugnai, W. Mrowczynski, R. Gurny, M. Möller and B. H. Walpoth, *Biomaterials*, 2012, **33**, 38-47.
19. V. Leszczak, K. C. Popat, *Journal of Biomedical Nanotechnology*, 2014 (accepted).
20. V. Leszczak, D. A. Baskett and K. C. Popat, *Journal of Functional Biomaterials*, 2014, **5**, 58-77.

21. V. Leszczak, B. S. Smith and K. C. Popat, *Journal of biomaterials science. Polymer edition*, 2013, **24**, 1529-1548.

22. K. C. Popat, J. R. Porter and A. Henson, *Biomaterials*, 2009, **30**, 780-788.

23. Y. Zhu and W. F. Ong, *Materials Science and Engineering: C*, 2009, **29**, 1046-1050.

24. S. In Jeong, S. Y. Kim, S. K. Cho, M. S. Chong, K. S. Kim, H. Kim, S. B. Lee and Y. M. Lee, *Biomaterials*, 2007, **28**, 1115-1122.

25. A. Wenger, A. Stahl, H. Weber, G. Finkenzeller, H. G. Augustin, G. B. Stark and U. Kneser, *Tissue engineering*, 2004, **10**, 1536-1547.

26. G. S. Jack, R. Zhang, M. Lee, Y. Xu, B. M. Wu and L. V. Rodríguez, *Biomaterials*, 2009, **30**, 3259-3270.

27. G. K. Owens, M. S. Kumar and B. R. Wamhoff, *Molecular Regulation of Vascular Smooth Muscle Cell Differentiation in Development and Disease*, 2004.

28. S. Sakurai, T. Fukasawa, J. M. Chong, A. Tanaka and M. Fukayama, *The American journal of pathology*, 1999, **154**, 23-28.

29. H.-C. Wu, T.-W. Wang, P.-L. Kang, Y.-H. Tsuang, J.-S. Sun and F.-H. Lin, *Biomaterials*, 2007, **28**, 1385-1392.

30. T. Ziegler, R. W. Alexander and R. M. Nerem, *Ann Biomed Eng*, 1995, **23**, 216-225.

31. A. Orlidge and P. A. D'Amore, *The Journal of Cell Biology*, 1987, **105**, 1455-1462.

TABLE CAPTIONS

Table 1 Surface elemental composition analyzed using XPS on different surfaces before and after collagen immobilization. Results indicate presence of N1s peaks after collagen immobilization.

FIGURE CAPTIONS

Figure 1 Representative SEM images of PCL and NW surfaces before and after collagen immobilization

Figure 2 Representative fluorescence microscopy images of EC and SMC co-cultures stained with Rhodamine Phalloidin (red) and DAPI (blue) on PCL, NW, colPCL and colNW surfaces. Experiments were replicated on at least three different samples with at least three different cell populations ($n_{min} = 9$).

Figure 3 Representative low (left) and high magnification (right) SEM images of SMC and EC co-cultures after 7 days of culture on different surfaces. Note: the surfaces were coated with a 10 nm layer of gold and imaged at 7 keV. Experiments were replicated on at least three different samples with at least three different cell populations ($n_{min} = 9$).

Figure 4 Western blot analysis of the expression of VE-cadherin, heavy chain myosin and non-muscle specific myosin IIb on different surfaces after 7 and 14 days in culture. Experiments were replicated with western blots with at least three different cell populations ($n_{min} = 9$, $p<0.05$)). In addition, after 14 days in culture, heavy chain myosin expression significantly decreases on NW, cPCL and cNW surfaces; and non-muscle specific myosin IIb expression significantly decreases on all surfaces.

Table 1

	PCL	cPCL	NW	cNW
C1s	74.5	72.3	74.5	74.7
N1s	0.0	7.1	0.0	3.4
O1s	25.5	20.6	25.5	21.9

Figure 1

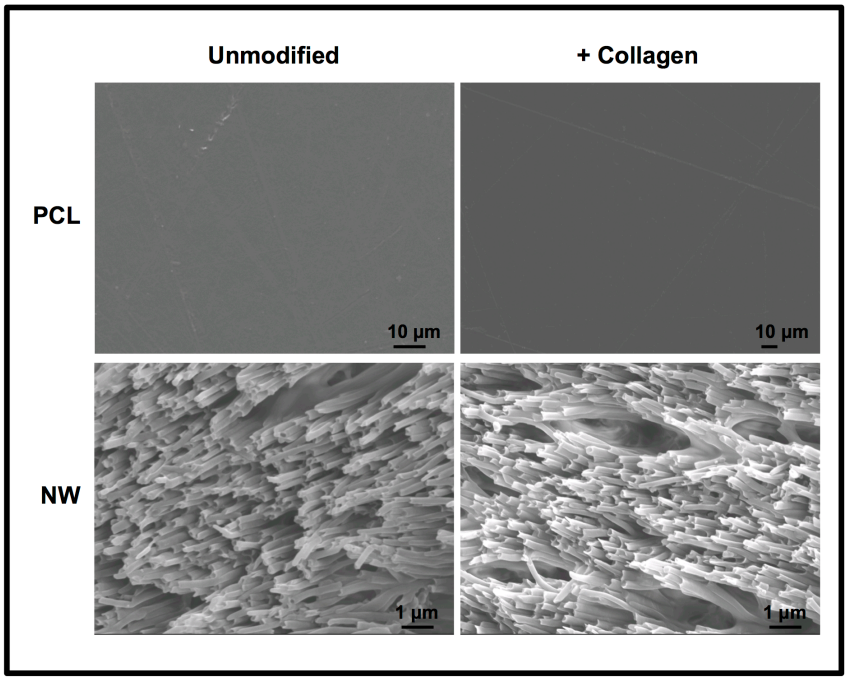

Figure 2

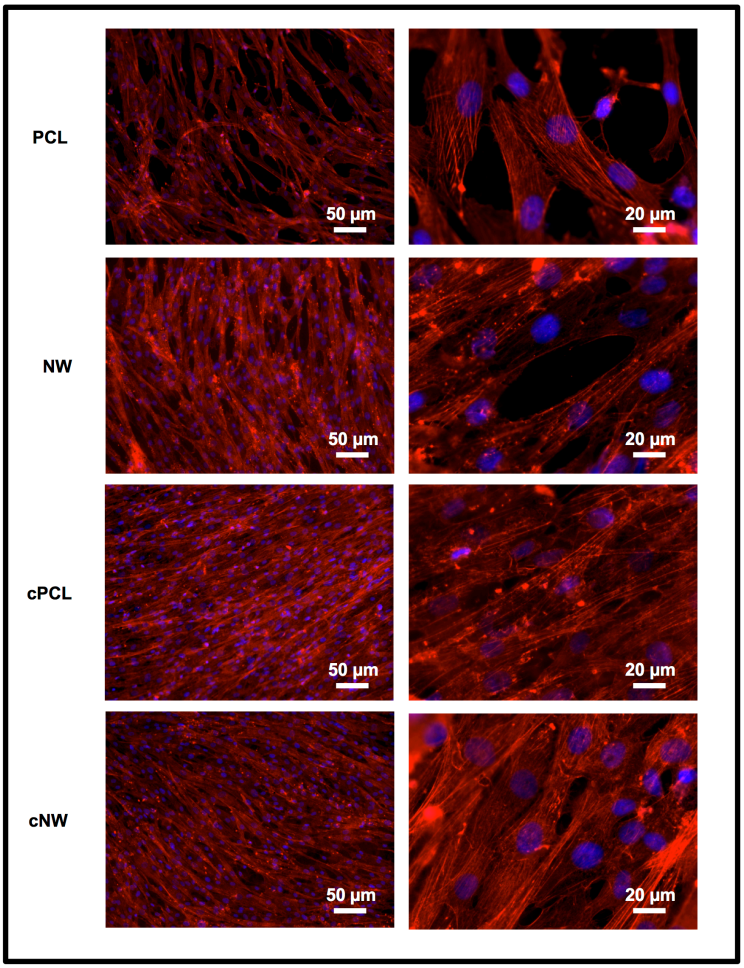

Figure 3

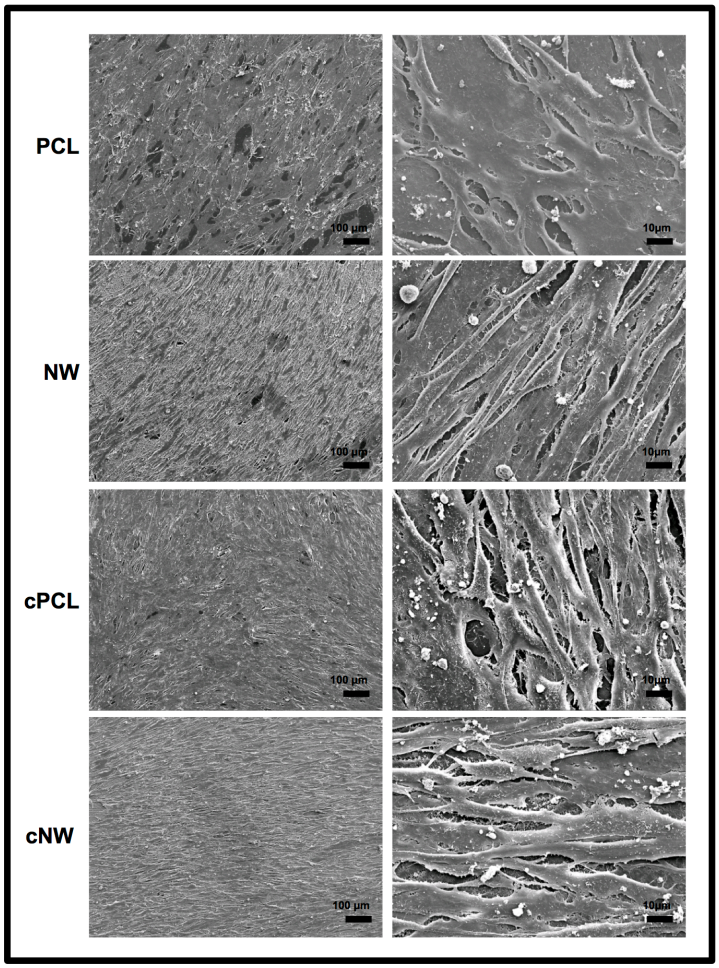

Figure 4